ELSEVIER

Chemical Engineering Journal 72 (1999) 245–252

Chemical Engineering Journal

Flow regimes and axial pressure profiles in a circulating fluidized bed

Won Namkung, Sung Won Kim, Sang Done Kim*

Department of Chemical Engineering and Energy and Environment Research Center, Korea Advanced Institute of Science and Technology, TaeJon 305-701, South Korea

Received 3 March 1998; received in revised form 10 November 1998; accepted 7 December 1998

Abstract

The hydrodynamics and flow regime in fast fluidized beds of FCC and silica sand particles were determined in a Plexiglas column (0.1 m i.d. × 5.3 m high). The transport velocity (U_{tr}) was determined by the emptying time and flooding point determination methods. At a given solid circulation rate, solid holdups in the upper dilute region exhibit their maximum values with variation of gas velocities, where a dense region forms at the bottom of the riser. The gas velocity at which solid holdup in the upper dilute region exhibits a maximum value is defined as the fast transition velocity (U_{FT}). The fast fluidization regime can be divided into the fast transition region and the fully developed fast fluidization region. A demarcation line between the two regions is proposed. The fast transition velocity and the transition velocity (U_{FD}) to pneumatic transport have been correlated. The transition velocity of the fast fluidization region can be predicted by the choking velocity, U_{FD} and U_{FT}.

Keywords: Flow regimes diagram; Fast fluidized bed; Fast transition velocity

1. Introduction

Fluidized bed reactors for gas–solid reaction have been widely used in chemical and petroleum industries. The bed has different flow regimes as a function of operating gas velocity [1]. Numerous studies have been carried out to define the flow regimes of bubbling and turbulent fluidization. However, studies on high velocity fluidization are comparatively sparse so that the hydrodynamics of high velocity fluidization are not well understood.

The fast fluidized bed regime has been defined by several ways during the last decade. Yerushalmi and Cankurt [2] defined the fast fluidization regime as the bed operated above the minimum transport velocity without choking with variation of solid circulation rate (G_s). Li and Kwauk [3] reported that the fast fluidized bed should have an inflection point that separating a dense phase at the bottom from a dilute phase at the top of the riser. Takeuchi et al. [4] claimed that the fast fluidized bed should contain both the dense and dilute entrained phases. The existence of the bottom dense region and the upper dilute region is common in the fast fluidized bed [5]. It has been observed that downward flow of solids near the wall region and upward flow of gas–solid through the core region in the upper dilute region of a circulating fluidized bed (CFB). Therefore, it has been claimed that the core-annulus flow structure exists in the upper dilute region of the CFB [6–8].

It is known that the solid holdup in the upper region (or freeboard) of the column exhibits a maximum value with variation of gas velocity at a given solid circulation rate [9,10]. Drahos et al. [9] explained that the gas velocity at which solid holdup in the upper dilute region exhibits a maximum value corresponds to the 'choking velocity'. However, this phenomenon has not been fully understood. Therefore, the hydrodynamic properties in the bottom dense and upper dilute regions in the bed should be determined to understand the flow regime transition. Also, the relationship between the variation of solid holdup in the upper and bottom regions in the bed should be determined. Most of the previous studies have been focused on the bottom dense region but studies on the upper dilute region are relatively sparse. In the present study, the hydrodynamics in the bottom and upper regions of the riser and flow regime in the fast fluidized bed have been determined using FCC and silica sand particles. The fast fluidization regime can be divided into the fast transition and fully developed fast fluidization regions based on U_{FT}. The fast transition velocity and the transition velocity (U_{FD}) to pneumatic transport in terms of Reynolds numbers have been correlated as a

*Corresponding author. Tel.: +82-42-869-3913; fax: +82-42-869-3910; e-mail: kimsd@cais.kaist.ac.kr

1385-8947/99/$ – see front matter
PII: S1385-8947(99)00013-3

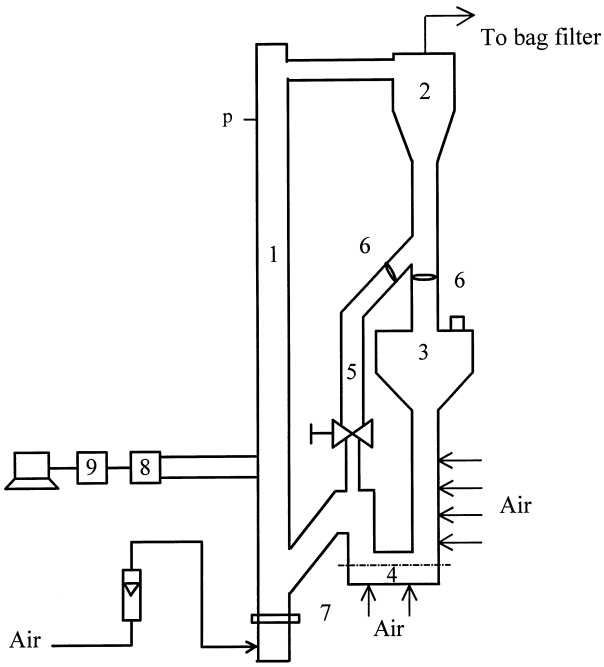

Fig. 1. Schematic diagram of the experimental apparatus. 1. riser, 2. cyclone, 3. hopper, 4. loop-seal, 5. measuring tube, 6. butterfly valve, 7. distributor, 8. pressure transducer, 9. Data 6000, p: pressure taps.

function of Archimedes number and a dimensionless group ($G_s/\rho_g U_t$).

2. Experimental details

Experiments were carried out in a Plexiglas column (0.1 m i.d. × 5.3 m height) as shown in Fig. 1. The solid particles used in this study were fluid catalytic cracking (FCC) catalyst and silica sand particles. The mean diameters of the FCC and silica sand particles are 65 and 125 μm, respectively, and their properties are shown in Table 1. The solid particles were supported on a perforated plate distributor situated between the main column section and an air box (0.1 m i.d. × 0.2 m height) into which air was fed through a pressure regulator, an oil filter and a calibrated flow meter. The exit configuration of the present system was a 90° take-off connector (0.04 m × 0.09 m) that located below 0.10 m from the top of the riser leading to the inlet of a cyclone. The entrained particles from the riser were collected by the primary and secondary cyclones and stored in a hopper. Solid particles from the hopper were transferred into a loop-seal through a downcomer (0.08 m i.d.) and were fed to the riser through a loop-seal that regulates solid circulation rate (G_s) by aeration. At steady state, the entire solids flow from two cyclones into a measuring column to determine solid circulation rate through the CFB loop. In the transparent measuring column, the descending time of particles along the known distance was measured [1,11]. With the knowledge of bulk density and the measured time, G_s can be determined. Pressure taps were mounted flush with the column wall and covered with a screen to prevent solid particles flowing out from the bed. The pressure transducers (Valydine P306D) were connected to pressure taps along the column height to measure pressure fluctuations between the different locations in the bed. The pressure signals from the pressure transducer were amplified and sent it via an A/D converter (Data 6000) to a personal computer for recording. The sampling interval of pressure fluctuation was selected at 10 ms and 4100 samples were collected for each experimental condition. From the pressure drop measurement, solid holdup (ε_s) was calculated at the given height.

Table 1
Physical properties of FCC and silica sand particles

Properties	FCC	Silica sand
Mean diameter (μm)	65	125
Apparent density (kg/m^3)	1720	3055
Terminal velocity (m/s)	0.19	0.88
Transport velocity (m/s)	1.40	2.40

3. Results and discussion

The transport velocity (U_{tr}) is the transition velocity between the turbulent and fast fluidized beds has been determined by various methods [1]. In this study, the U_{tr} is determined by the emptying time and flooding point determination methods [2]. With the emptying time method, the time required for all FCC or silica sand particles to leave the bed as a function of gas velocity (U_g) is considered as shown in Fig. 2. As U_g is increased, the bed material could be emptied in a short period of time due to sharp increase of particle carryover in the absence of solid recycle. As can be seen, two lines have different slopes at lower and higher U_g. From the intersection of these two lines, U_{tr} of the particles can be determined [12,13]. As can be seen in Fig. 2(A), the initial solid weight does not affect the U_{tr}. That is a necessary intrinsic condition to employ this method to determine U_{tr} [1]. The resulting values of U_{tr} are found to be 1.40 and 2.40 m/s for FCC and silica sand particles, respectively.

The relationship between volumetric gas flow rate [$U_g = \varepsilon(U_g/\varepsilon)$] and solid volumetric flux [$(1-\varepsilon)U_s = G_s/\rho_s$] is shown in Fig. 3. The intersection between the lines in Fig. 3 represents a flooding point that corresponds to the transport velocity [2]. As can be seen, the resulting U_{tr} values are 1.44 and 2.52 m/s for FCC and silica sand particles, respectively. These are similar to the U_{tr} values from the emptying time method (Fig. 2). These U_{tr} values obtained are well in accordance to the values derived from the correlations of Perales et al. [13] and Lee and Kim [14] for FCC and silica sand particles, respectively.

The axial solid holdup distributions of silica sand particles with variations of U_g and G_s are shown in Fig. 4 where

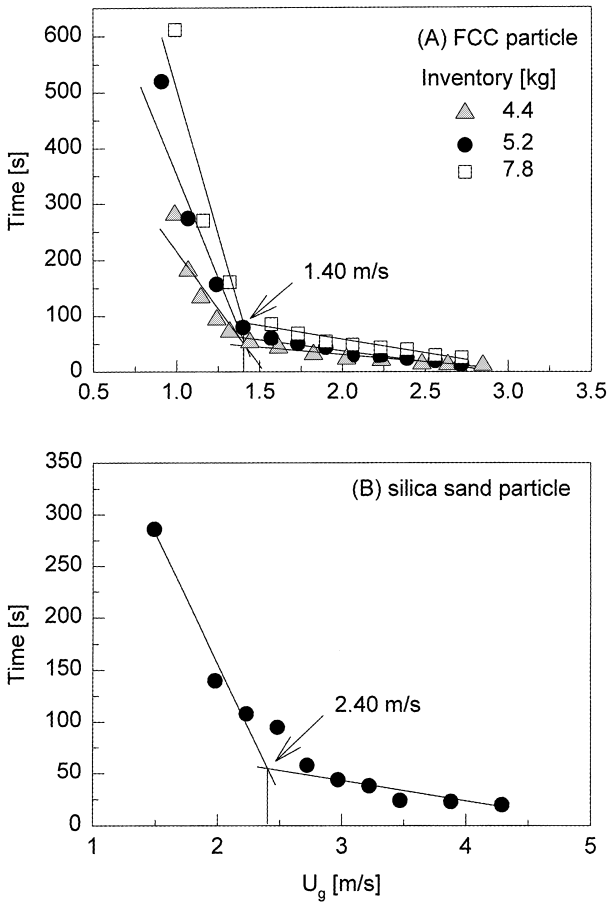

Fig. 2. Time required for all the particles to leave the bed as a function of gas velocity.

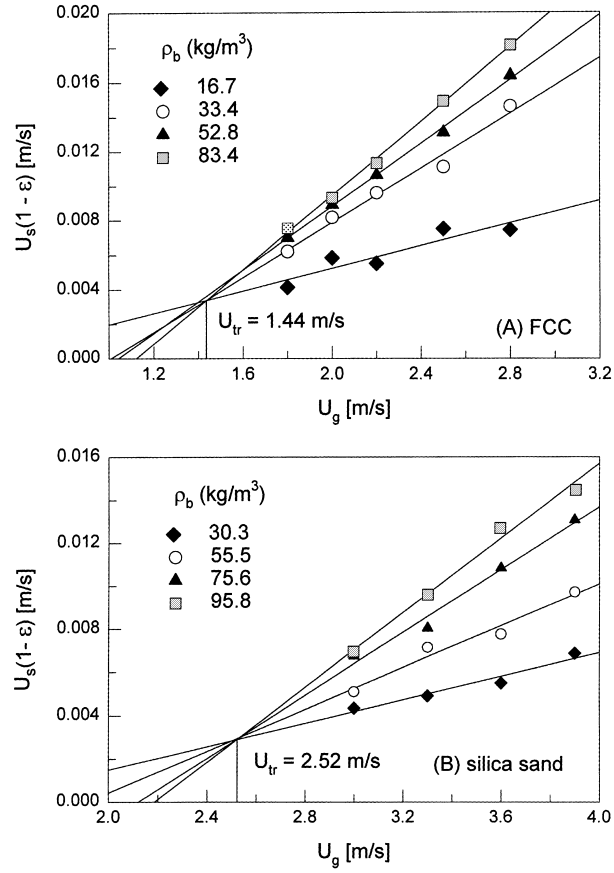

Fig. 3. Volumetric flux of solid with variation of gas velocities at constant bed densities.

solid holdup (ε_s) in the riser decreases with increasing U_g due to the increase of particle entrainment rate (Fig. 4(A)). At a given U_g, ε_s in the riser increases with increasing G_s (Fig. 4(B)). At lower G_s, the axial ε_s distribution in the whole column becomes uniform and exhibits a similar ε_s value in the dilute pneumatic transport flow with solids reflux in the wall region [15]. As G_s is increased, a condition is reached at which U_g is insufficient to entrain all the solids entering into the riser without solid accumulation at the bottom of the riser so that solid particles begin to accumulate at the bottom of the riser to form a dense phase. The riser then contains a dense phase transport region topped by a region of dilute-phase refluxing transport. As can be seen in Fig. 4(A), if the bed operates in bubbling or turbulent flow regime ($G_s = 0$), a distinct bed surface separating the dense region in the lower part of the bed and the dilute (freeboard) zone in the upper part of the bed was observed at lower U_g. In bubbling and turbulent fluidization regimes at the bottom region of the riser, ε_s values are much higher than those in high velocity fluidization regime at the bottom region of the riser. Whereas, ε_s values in bubbling and turbulent fluidization regimes are much lower than those ε_s in high velocity fluidization regime at the upper part (or freeboard) of the riser due to the increase of particle entrainment from the bottom dense to the upper dilute regions with increasing U_g.

The effect of U_g on ε_s in the upper dilute region, where ε_s keeps almost constant value along the column height, is shown in Fig. 5. ε_s exhibits a maximum value at a given G_s with variation of U_g. Solid phase holdup (ε_s) of FCC is higher than that of silica sand particles at the similar experimental conditions since entrainment rate of FCC is higher than that of silica sand particles at the similar experimental conditions. At very low U_g, ε_s in the upper region of the riser is approximately zero. As U_g is increased, ε_s in the upper region increases due to the increase of particle entrainment from the bed surface to the freeboard. However, ε_s in the bottom and upper regions of the riser decreases since particle carryover increases with a further increase in U_g without dense region formation at the bottom of the riser. The gas velocity at which ε_s exhibit its maximum values in the upper dilute region has not been fully understood. As can be seen in Fig. 5(C), Drahos et al. [9] explained the gas velocity at which ε_s in the upper dilute region exhibits its maximum values corresponding to the choking velocity in their very limited experimental conditions ($U_g = 1$–2 m/s, $G_s = 2.0$–5.5 kg/m^2 s). Bai et al. [10] proposed that U_g corresponding to the peak of ΔP_u is

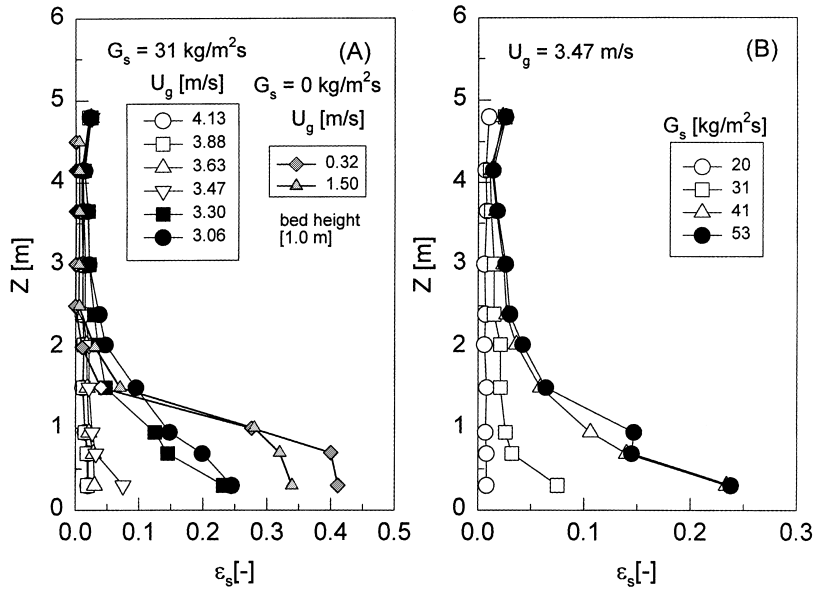

Fig. 4. Effects of gas velocity and solid circulation rate on the axial solid holdup distribution.

regarded as the transition velocity (U_{tr}) between the turbulent and fast fluidization without presenting their experimental data.

Variation of ε_s with U_g in the upper and bottom of the riser at a constant G_s for silica sand particles is shown in Fig. 6. As can be seen, ε_s in the upper dilute region exhibits maximum values with variation of U_g at the different riser heights. When U_g is very high, ε_s in the riser is very low and the difference in ε_s between the bottom and upper regions is negligibly small except at the exit region where ε_s is affected by the exit structure [10,16]. With an abrupt exit structure, the entrained particles are separated when the particle laden gas impact onto the top dead end of the riser so that there is a considerable internal particle reflux along the riser walls, and consequent increase in ε_s in the top section of the riser [10,16]. As can be seen, ε_s in the exit region reaches a saturation value or decreases slightly with increasing U_g. As U_g is decreased, ε_s increases and particles start to accumulate at the bottom of the riser (Fig. 6(B)). It has been observed that a dense region forms at the bottom of the riser when ε_s exhibits a maximum value in the upper dilute region. In the dense region, ε_s varies slightly with U_g but the effect of G_s on ε_s is very small as in the condition of the saturation carrying capacity defined by Bai and Kato [17]. However, their definition [17] is different from the traditional definition in the literature [18–20].

In the present study, the gas velocity at which ε_s exhibits a maximum value in the upper region of the riser is defined as the fast transition velocity (U_{FT}) that lies between the transport velocity (U_{tr}) and the transition velocity (U_{FD}) to pneumatic transport.

As a result, three different stages in the upper dilute region with variation of U_g can be identified as

1. $U_g > U_{FT}$: Above U_{FD}, solid particles traverse the bed in the fully entrained flow, thus ε_s increases with decreasing U_g. If U_g decreases further below U_{FD}, particles start to accumulate at the bottom of the riser.
2. $U_g = U_{FT}$: ε_s in the upper dilute region exhibits a maximum value and dense bed forms in the bottom region. Typical axial ε_s distribution exists such as the bottom dense, upper dilute and a transition region between dense and dilute regions.
3. $U_g < U_{FT}$: ε_s in the upper region of the riser decreases with decreasing U_g since particle entrainment rate decreases with decreasing U_g. ε_s in the bottom dense region increases slightly with decreasing U_g.

The effect of U_g on ε_s and the standard deviation of pressure fluctuation with FCC particles is shown in Fig. 7. In the bubbling and turbulent flow regimes, pressure fluctuations are largely affected by the bed density and bubble properties. However, bubbles are no further existing in the fast fluidized bed. Therefore, standard deviation of pressure fluctuations is solely determined by apparent ε_s in the fast fluidized bed. As can be seen, the standard deviation decreases with increasing U_g in the bottom region. While the standard deviation in the upper region exhibits a maximum value with variation of U_g. It can be anticipated that standard deviation of pressure fluctuation varies similarly to ε_s with variation of U_g.

3.1. Correlations

The transition velocity (U_{FD}) to pneumatic transport in terms of Reynolds number has been correlated with Archimedes number and a dimensionless group with the data of

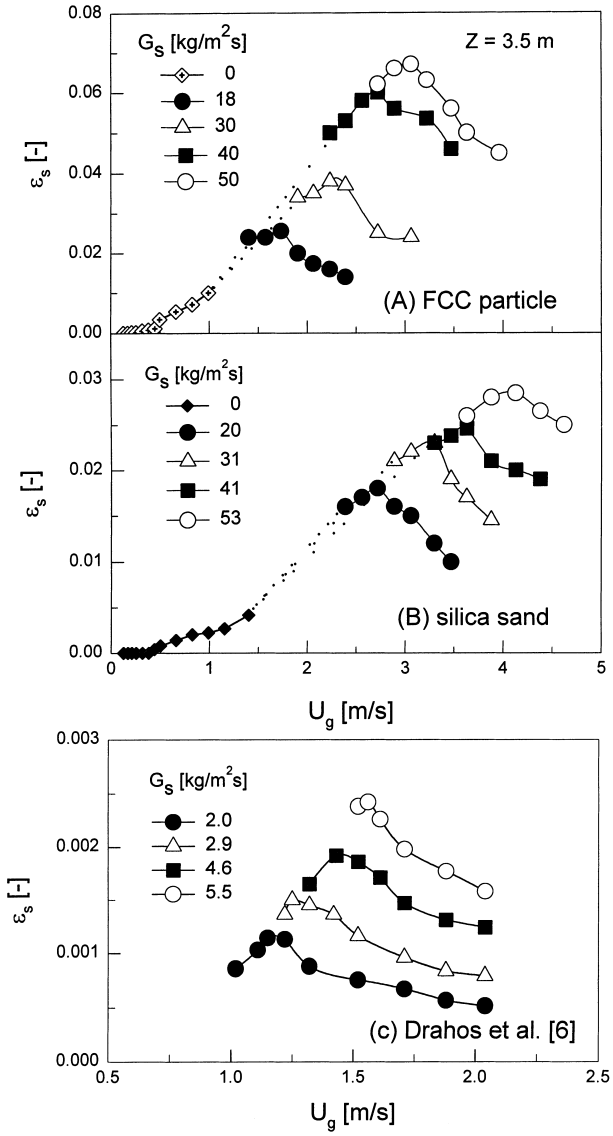

Fig. 5. Effect of gas velocity on solid holdup in the upper dilute region.

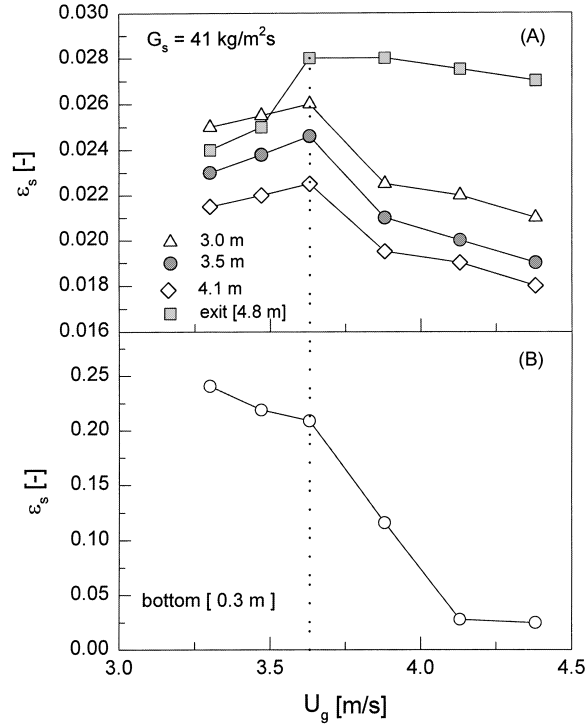

Fig. 6. Effect of gas velocity on solid holdup at a constant solid circulation rate of silica sand particles.

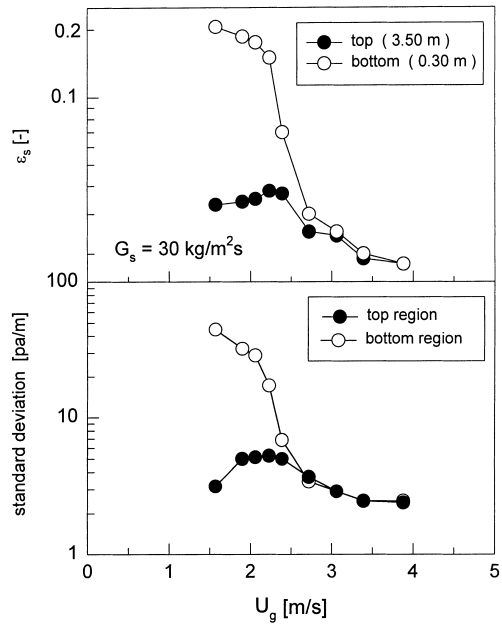

Fig. 7. Effect of gas velocity on solid holdup and standard deviation of pressure fluctuation of FCC particles.

the present and previous studies [3,4,21–23] as

$$\mathrm{Re_{FD}} = 0.440\,\mathrm{Ar}^{0.563}\left(\frac{G_s}{\rho_g U_t}\right)^{0.359} \quad (1)$$

with a correlation coefficient of 0.991 and a standard deviation of 0.190. Eq. (1) covers the range of variables $5 \leq \mathrm{Ar} \leq 1170$ and $1.0 \leq (G_s/\rho_g U_t) \leq 5 \times 10^4$.

Bai and Kato [17] proposed a correlation to determine the saturation carrying capacity that is equivalent to the fast transition velocity (U_{FT}) in this study. As can be seen in Fig. 8, their correlation predicts U_{FT} well for FCC particles that is classified as the Geldart group A but, it significantly underestimates U_{FT} for silica sand particles in this study.

The U_{FT} values in terms of Reynolds number in the present and previous studies [3,4,17,19,22,24–27] have been correlated as a function of Archimedes number and a dimensionless group as

$$\mathrm{Re_{FT}} = 0.395\,\mathrm{Ar}^{0.572}\left(\frac{G_s}{\rho_g U_t}\right)^{0.345} \quad (2)$$

with a correlation coefficient of 0.967 and a standard deviation of 0.188. This correlation covers the range of

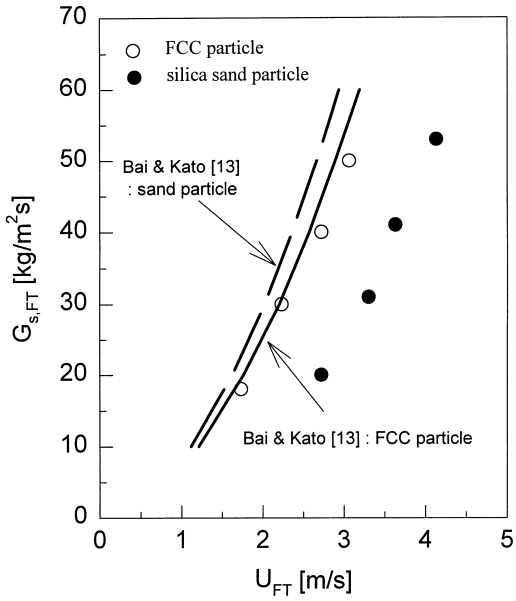

Fig. 8. Comparison between the measured and calculated values of U_{FT}.

Table 2
Summary of the experimental conditions used in the correlation

Workers	Solids	Particle size (μm)	Particle density (kg/m^3)
Bai and Kato [17]	FCC	51.9	1623
Bi et al. [21]	Silica gel	280	706
	Silica gel	140	710
	FCC	48	1473
Gao [24]	FCC	62	1020
	Silica gel	205	760
	AN catalyst	82	1780
Hirama et al. [23]	High alumina	38	750
Li and Kwauk [3]	Alumina	81	3090
	Pyrite cinder	56	3050
	Iron concentrate	105	4510
	FCC	58	1780
Li et al. [19]	FCC	54	930
Nishino [25]	FCC	69	1690
Ouyang and Potter [27]	FCC	65	1380
Rhodes and Geldart [22]	9G alumina	64	1800
	Alumina 25	42	1020
	CBZ-1	38	1310
Takeuchi et al. [4]	FCC	57	1080
Yang and Sun [26]	Silica gel	165	794
This study	FCC	65	1720
	Silica sand	125	3055

variables $2.5 \leq \mathrm{Ar} \leq 930$ and $17.0 \leq (G_s/(\rho_g U_t) \leq 1040$. The details of experimental conditions of the present and previous studies are summarized in Table 2.

3.2. Flow regime map

The flow regime map for FCC and silica sand particles in the riser is shown in Fig. 9. As can be seen, the fast fluidized bed exists between the captive beds (bubbling and turbulent)

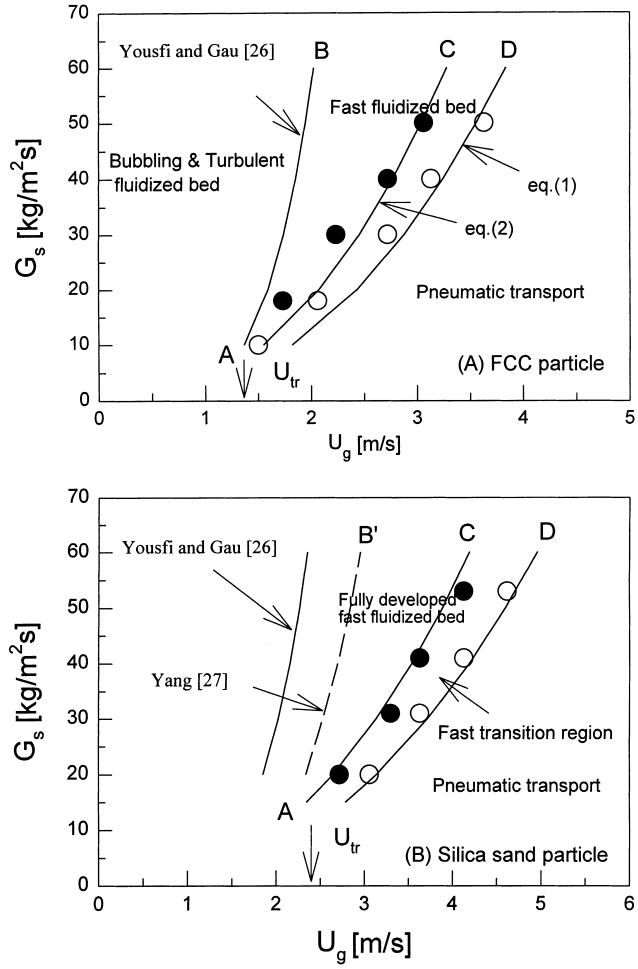

Fig. 9. Flow regime diagram in a CFB of FCC and silica sand particles.

and pneumatic transport. The boundary between the batch at lower U_g and circulating fluidized beds at higher U_g is not well defined and far from being fully understood. The transition from the turbulent to fast fluidization regions may occur when significant amounts of particles are entrained from the fluidized bed [28]. The estimated U_{tr} is the minimum condition of transition velocity between the turbulent and fast fluidization regimes [5]. Biswas and Leung [29] found that transition from turbulent to fast fluidization with FCC particles can be predicted by the choking correlation of Yousfi and Gau [30]. This concept has been further explored by Reddy Karri and Knowlton [5] and Bi and Grace [31]. Thus, the curve AB in Fig. 9(A) can be calculated from the correlation of Yousfi and Gau [30] for FCC particles. Later, Bi and Grace [31] extended the correlation of Yousfi and Gau [30] as the boundary condition between the turbulent and fast fluidization regimes for Geldart group B particles. However, the choking correlation of Yousfi and Gau [30] underestimates the transition line between the turbulent and fast fluidized beds of silica sand particles in this study (Fig. 9(B)). The calculated values from the correlation of Yousfi and Gau [30] is very low compared to U_{tr} that is the transition velocity between

turbulent and fast fluidization. As can be seen, U_{tr} for silica sand particles can be predicted well by the choking correlation of Yang [32] compared to the correlation of Yousfi and Gau [30]. Indeed, further studies are needed for verification.

The curve AD represents the boundary between the fast fluidization and pneumatic transport [4]. The solids circulation rate at this curve is the maximum attainable rate at a given U_g without solids accumulation. The solids circulation rate at this curve therefore, appears to be the same as the saturation carrying capacity [18]. Therefore, fast fluidized bed can be predicted by the curves AB and AD.

The existence of bottom dense region and upper dilute region is common in the fast fluidized bed [5]. Although the axial solid holdup distribution is formed by the variation of U_g, dense region in the bottom of the riser may not be formed at a certain operating conditions. This condition exists between the curves AB and AD. However, this condition is different from the general definition of fast fluidization proposed by Li and Kwauk [3]. Therefore, the flow regimes in this condition should be clarified. It has been seen that dense region forms in the bottom of the riser when ε_s exhibits the maximum value in the upper dilute region (Fig. 6). Based on U_{FT}, fast fluidization region can be divided into two regions depending on the operating conditions. One case is the S-shaped solid holdup profile or fully developed fast fluidization region that may indicate dense bed formation in the bottom of the riser. In this region, typical axial solid holdup distribution exists with a transition between the bottom dense and the upper dilute region. If U_g is constant at this condition (Fig. 4B), ε_s in the bottom dense region is not largely affected by the further increase of G_s ($41 \rightarrow 53$ kg/m^2 s). This fully developed fast fluidization region lies between the curves AB and AC that is the similar definition proposed by Li and Kwauk [3]. The other one is the fast transition region defined in this study. Although the axial ε_s distribution exists, the dense bed in the bottom region is not formed. As can be seen in Fig. 4(B), ε_s in the bottom region increases with increasing G_s from 31 to 41 kg/m^2 s. Therefore, ε_s in the bottom region is largely affected by variation of G_s in the region between the curves AC and AD in Fig. 9. Also, Bai and Kato [17] divided the fast fluidization into two regions, namely a S-shaped and an exponential profile of ε_s based on U_{FT} and $G_{s,\,FT}$. However, the S-shaped ε_s profile is not observed with the different experimental apparatus and operating conditions [33,34] even with the dense bed formation in the bottom region of the riser. Therefore, in this study, fast fluidization region can be divided into two regions based on U_{FT} at a given G_s, namely the fully developed fast fluidization and fast transition regions as represented by the curve AC in Fig. 9 where the curves AD and AC are calculated from Eqs. (1) and (2), respectively. As can be seen, the calculated values are in well accordance with the experimental values for FCC and silica sand particles. Therefore, the locus of boundary to predict the fast fluidized bed may be determined by the choking correlations in the literature [30,32], Eqs. (1) and (2).

4. Conclusions

The transport velocities (U_{tr}) of FCC and silica sand particles are found to be 1.40 and 2.40 m/s, respectively. The solid holdups in the upper dilute region exhibit maximum values with variation of U_g. The fast transition velocity (U_{FT}) corresponds to the gas velocity at which the dense region forms in the bottom of the riser. The fast fluidization regime can be divided into the fast transition regions and the fully developed fast fluidization and based on U_{FT}. The fast transition velocity (U_{FT}) and the transition velocity (U_{FD}) to pneumatic transport in terms of Reynolds numbers have been correlated as a function of Archimedes number and a dimensionless group ($G_s/\rho_g U_t$). The transition velocity of fast fluidization regions can be determined by the choking velocity, U_{FD} and U_{FT}.

Appendix

Nomenclature

Ar	Archimedes number, $d_p^3 \rho_g(\rho_s - \rho_g)g/\mu^2$ (-)
d_p	Particle diameter (m)
G_s	Circulation rate of solids (kg m^{-2} s^{-1})
$G_{s,\,FT}$	Circulation rate of transition solids between fully developed fast fluidized bed and fast transition region (kg m^{-2} s^{-1})
L	Column length (m)
Re	Reynolds number, $\rho_g d_p U/\mu$ (-)
U_{FD}	Transition gas velocity between fast fluidized bed and pneumatic transport (m s^{-1})
U_{FT}	Fast transition velocity (m s^{-1})
U_g	Superficial gas velocity (m s^{-1})
U_s	Velocity of the solids (m s^{-1})
U_t	Particle terminal velocity (m s^{-1})
U_{tr}	Transport velocity (m s^{-1})
ΔP_u	Pressure drop in upper part of column (pa)
ε_s	Average solid holdup (-)
ε	Average gas holdup (-)
ρ_g	Gas density (kg m^{-3})
ρ_s	Particle density (kg m^{-3})
μ	Gas viscosity (kg m^{-1} s^{-1})

References

[1] J. Adanez, L.F. de Diego, P. Gayan, Powder Technol. 77 (1993) 61–68.
[2] J. Yerushalmi, N.T. Cankurt, Powder Technol. 24 (1979) 187–205.
[3] Y. Li, M. Kwauk, in: J.R. Grace, J.M. Matsen (Eds.), Fluidization, Plenum Press, New York, 1980, pp. 537–544.

[4] H. Takeuchi, T. Hirama, T. Chiba, J. Biswas, L.S. Leung, Powder Technol. 47 (1986) 195–199.
[5] S.B. Reddy Karri, T.M. Knowlton, in: P. Basu, M. Horio, M. Hasatani (Eds.), Circulating Fluidized Bed Technology III, Pergamon Press, New York, 1991, pp. 67–72.
[6] D. Geldart, M.J. Rhodes, in: P. Basu (Eds.), Circulating Fluidized Bed Technology, Pergamon Press, New York, 1986, pp. 21–31.
[7] W. Zhang, Y. Tung, F. Johnsson, Chem. Eng. Sci. 46 (1991) 3045–3052.
[8] W. Namkung, S.D. Kim, Powder Technol. 99 (1998) 70–78.
[9] J. Drahos, J. Cermak, R. Guardani, K. Schugerl, Powder Technol. 56 (1988) 41–48.
[10] D. Bai, Y. Jin, Z. Yu, Chem. Eng. Technol. 16 (1993) 303–313.
[11] M.J. Rhodes, P. Laussmann, Can. J. Chem. Eng. 70 (1992) 625–630.
[12] G.Y. Han, G.S. Lee, S.D. Kim, Korean J. Chem. Eng. 2 (1985) 141–147.
[13] J.F. Perales, T. Coll, M.F. Lop, L. Puigjaner, J. Arnaldos, J. Casal, in: P. Basu, M. Horio, M. Hasatani (Eds.), Circulating Fluidized Bed Technol. III, Pergamon Press, Oxford, 1991, pp. 73–78.
[14] G.S. Lee, S.D. Kim, Powder Technol. 62 (1990) 207–215.
[15] Y.J. Cho, W. Namkung, S.D. Kim, S. Park, J. Chem. Eng. Jpn 27 (1994) 158–164.
[16] W. Namkung, Y.J. Cho, S.D. Kim, Hwahak Konghak 32 (1994) 241–247.
[17] D. Bai, K. Kato, J. Chem. Eng. Jpn 28 (1995) 179–185.
[18] F.A. Zenz, N.A. Weil, AIChE J. 4 (1958) 472–479.
[19] J. Li, Y. Tung, M. Kwauk, in: J.F. Large, P. Basu (Eds.), Circulating Fluidized Bed Technology II, Pergamon Press, Oxford, 1988, pp. 193–203.
[20] H.T. Bi, J.R. Grace, X.Y. Zhu, Int. J. Multiphase Flow 19 (1993) 1077–1092.
[21] H.T. Bi, Y. Jin, D. Jiang, J. Chem. Ind. Eng. (China) 41 (1991) 623.
[22] M.J. Rhodes, D. Geldart, in: P. Basu (Eds.), Circulating Fluidized Bed Technol., Pergamon Press, New York, 1986, pp. 193–200.
[23] T. Hirama, T. Takeuchi, T. Chiba, Powder Technol. 70 (1992) 215–222.
[24] S. Gao, Master thesis, Shenyang Research Institute of Chemical Engineering, China, 1990.
[25] K. Nishino, Master thesis, Gunma university, Japan, 1990.
[26] G.L. Yang, J.K. Sun, in: M. Kwauk, M. Hasatani (Eds.), Fluidization 1991, Science and Technology, Science Press, Beijing, 1991, pp. 37–45.
[27] S. Ouyang, O.E. Potter, Ind. Eng. Chem. Res. 32 (1993) 1041–1045.
[28] H.T. Bi, J.R. Grace, J.X. Zhu, Chem. Eng. Des. Dev. 73 (1995) 154–161.
[29] J. Biswas, L.S. Leung, Powder Technol. 51 (1987) 179–180.
[30] Y. Yousfi, G. Gau, Chem. Eng. Sci. 29 (1974) 1939–1946.
[31] H.T. Bi, J.R. Grace, Int. J. Multiphase Flow 21 (1995) 1229–1236.
[32] W.C. Yang, Powder Technol. 35 (1983) 143–150.
[33] U. Arena, A. Cammarota, L. Pistone, in: P. Basu (Eds.), Circulating Fluidized Bed Technology, Pergamon Press, New York, 1986, pp. 119–125.
[34] D.R. Bai, Y. Jin, Z.Q. Yu, J.X. Zhu, Powder Technol. 71 (1992) 51–58.